

Examining Transport and Integrated Modeling Predictive Capabilities for Negative-Triangularity Scenarios

J. McClenaghan¹, A. Marinoni², L.L. Lao¹, G.M. Staebler¹, S.P. Smith¹, O.M. Meneghini¹,

B.C. Lyons¹, P.B. Snyder³, and M. Austin⁴

¹*General Atomics, PO Box 85608, San Diego, CA 92186–5608, USA*

²*Massachusetts Institute of Technology, Cambridge, Massachusetts 02139, USA*

³*Oak Ridge National Laboratory, Oak Ridge, Tennessee 37831, USA*

⁴*The University of Texas at Austin, Austin, Texas 78712, USA*

High energy confinement (τ_e) is required for a steady-state fusion reactor [1]. High confinement is typically achieved in positive triangularity (δ) H-mode plasmas. Positive- δ has long been known to improve both confinement and stability. However, the improvement in confinement from the H-mode pedestal typically is accompanied by edge localized modes, which produce large spikes in energy flux that can erode the divertor. Experiments on TCV [2] and DIII-D [3] have shown that L-mode confinement improves dramatically in a negative- δ shape. Two similar DIII-D discharges with matched values for major radius, minor radius, and elongation, but opposite $\delta = -0.4, 0.4$ were compared. The plasmas were heated with up to 10 MW of neutral beam injection (NBI) power and up to 3 MW of electron cyclotron heating (ECH) power and had high levels of confinement.

The earliest modeling of transport of negative- δ suggested that trapped electron modes (TEM) could be suppressed by negative- δ [4]. Gyrokinetic simulations of TCV discharges suggested that trapped electron modes were suppressed in negative- δ compared to the positive- δ counterpart [5]. Exploration of negative- δ showed that negative- δ has reduced transport compared to positive- δ [6], and suggested negative- δ may increase the critical gradient leading to improved transport [7].

The predictive capabilities of TGYRO [8] find that predicted profiles of electron temperature (T_e), ion temperature (T_i), electron density (n_e), and $E \times B$ shear (ω) agree reasonably well in both negative- δ and positive- δ at low auxiliary powers (< 5 MW). TGYRO is analyzed for a positive- δ and a negative- δ plasma heated with $P_{EC} = 2$ MW and $P_{NBI} = 2$ MW with a fixed boundary condition for the kinetic profiles in these simulations is set to the experimental values at $\rho = 0.8$. Figure 1 shows the experimental profile fits and the TGYRO predicted profiles of T_i , T_e , n_e , and ω in positive- δ and negative- δ . Experiments and TGYRO predictions both

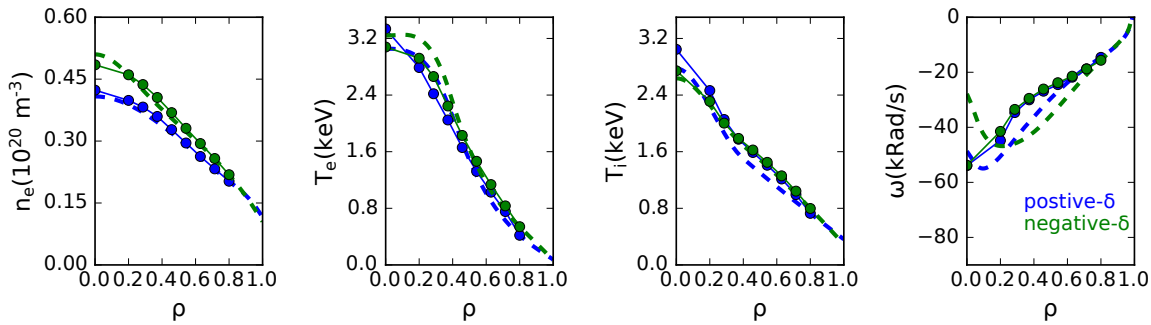


Figure 1: *TGYRO prediction (solid) of n_e , T_e , T_i , and ω and experimental profile fits (dashed) in NBI+ECH heated plasmas in positive- δ (blue) and in negative- δ (green).*

have higher values for n_e and T_e are observed in negative- δ compared to positive- δ . The T_e profile is slightly underpredicted for both positive- δ and negative- δ . The T_i profile is slightly overpredicted ($\sim 10\%$) for positive- δ , while it is almost perfectly predicted in negative- δ .

Analysis of the turbulent transport using the quasilinear gyro-Landau fluid code TGLF [9] is performed. TGLF predicts a large difference in particle flux (Γ) between positive- δ and negative- δ as a function of temperature gradient scale length a/L_{T_e} , as shown in Figure 2. Here, a is the minor radius, $1/L_{T_e} = \partial T_e / \partial r / T_e$. As a/L_{T_e} is increased, the predicted Γ for the negative- δ scenario becomes negative. This is opposite to the predicted flux in the positive- δ scenario where Γ increases as a/L_{T_e} moves away from the experimental gradient. This difference in particle transport behavior could possibly lead to better confinement for negative- δ with negative- δ having better higher experimental n_e and T_e in Figure 2.

Core-pedestal modeling shows confinement and β_N improve at negative δ and at positive δ . Similar parameters to the DIII-D experiment of $\beta_N = 2$, $n_{e,ped} = 0.35 \times 10^{20} \text{ m}^{-3}$, $\kappa = 1.6$, $B_t = 2 \text{ T}$, and $I_p = 0.8 \text{ MA}$ are used. Modeling is done using the STEP [10] module in OMFIT [11], which iterates between TGYRO[8], ONETWO [12], and CHEASE [13]. TGYRO is used to predict kinetic profiles. ONETWO is used to predict the current evolution. CHEASE is used

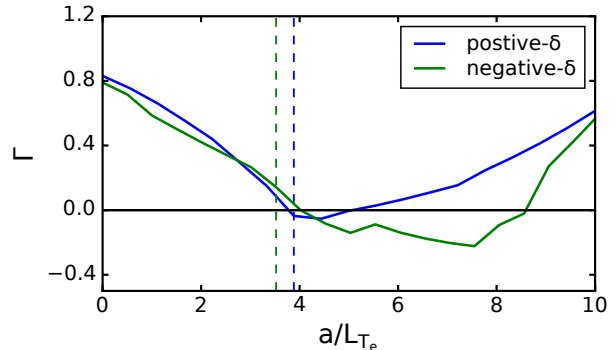


Figure 2: *TGLF-SAT0 predicted Γ ($10^{20} \text{ m}^{-2} \text{ s}^{-1}$) at $\rho = 0.6$ for a positive- δ and negative- δ ECH only plasma plotted vs. a/L_{T_e} . The vertical dashed lines indicate the experimental scale lengths.*

to ensure Grad-Shafranov is satisfied with a Miller geometry. The current is evolved assuming the current fully penetrates to steady-state from neoclassical resistivity. An additional radially constant current diffusion is applied where $q < 1$ to raise the on-axis q just above unity. A radially uniform $Z_{eff} = 1.7$ is used. Fixed Gaussian sources of electron heating are used, one located at $\rho = 0.6$ and the other at $\rho = 0.0$ to represent electron cyclotron heating. The pedestal boundary condition is taken to be the EPED [14] prediction with $\beta_N = 2$ shown in Figure 3. The pedestal height increases monotonically with increasing δ . While H-mode has rarely been observed experimentally for strong negative- δ potentially prevented due to ballooning modes [15], we still use EPED to set the edge conditions for negative triangularity as EPED has been shown to accurately predict negative- δ plasma down to $\delta = -0.2$ [16]. Using EPED below $\delta = -0.2$ gives a reduction in edge confinement at negative- δ without needing different edge models for negative- δ and positive- δ . TGLF-SAT0 is used in TGYRO with settings for electrostatic and using the $E \times B$ quench rule.

The STEP predicted confinement improvement at negative- δ is predicted to be stronger at high power densities and with strong electron heating sources. Figure 3 shows STEP predicted β_N vs triangularity for two injected powers: 10 MW and 20 MW, and NBI only and a 50/50 mix of NBI+ECH. At $P_{aux} = 10$ MW for both heating types, modest improvements in β_N are predicted with simulations when δ is decreased from $\delta = -0.2$ to $\delta = -0.6$. For the 50/50 mix of NBI+ECH heating, the STEP prediction of β_N becomes U-shaped at $P_{aux} = 20$ MW with positive- δ with $\beta_{N,\delta=-0.6} \sim \beta_{N,\delta=0.6}$. The increase in β_N at negative- δ compared to positive- δ is stronger for NBI+ECH than with NBI only. However, all values of β_N are lower than the NBI only prediction.

The transport and integrated modeling predictive capabilities of the negative- δ scenario are examined in which TGYRO predicts stronger n_e and T_e gradients in negative- δ compared to positive- δ , consistent with the experiment. TGLF predicts that increasing electron temperature gradient scale length reduces the particle transport in negative- δ . This suggests that electron heating may not degrade core plasma particle confinement the way positive- δ does. The predicted confinement improvement at negative- δ from core-pedestal modeling is stronger in high

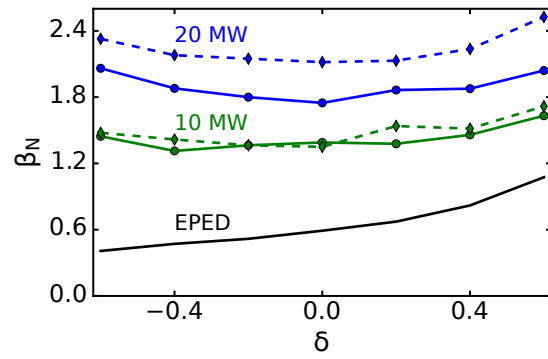


Figure 3: STEP predicted β_N NBI only (dashed) and NBI+ECH (solid) heating $P_{aux} = 10$ MW (blue) and $P_{aux} = 20$ MW (green) with EPED boundary (black).

power electron heated plasmas.

References

- [1] C. Gormezano et al. *Nucl. Fusion*, 47(6), 2007.
- [2] Y Camenen et al. *Nucl. Fusion*, 47(7):510–516, 2007.
- [3] M. E. Austin et al. *Phys. Rev. Lett.*, 122, 2019.
- [4] G. Rewoldt, W. M. Tang, and M. S. Chance. *Phys. Fluids*, 25(3), 1982.
- [5] A Marinoni. *Plasma Phys. Control. Fusion*, 51(5), 2009.
- [6] G. Merlo et al. *Phys. Plasmas*, 26(10), 2019.
- [7] G Merlo et al. *Plasma Phys. Control. Fusion*, 57(5), 2015.
- [8] J. Candy et al. *Phys. Plasmas*, 16(6), 2009.
- [9] G. M. Staebler et al. *Phys. Plasmas*, 14(5), 2007.
- [10] O. Meneghini et al. *Nucl. Fusion*, 61(2), 2020.
- [11] O. Meneghini et al. *Nucl. Fusion*, 55(8), 2015.
- [12] H.St. John et al. *15th International Conference on Plasma Physics and Controlled Nuclear*, 1, 1994.
- [13] O. Sauter et al. *Phys. Plasmas*, 4, 1997.
- [14] P.B. Snyder and other. *Nucl. Fusion*, 51:103016, 2011.
- [15] S. Saarelma et al. *Plasma Phys. Control. Fusion*, 63(10), 2021.
- [16] A. Merle et al. *Plasma Physics and Controlled Fusion*, 59(10):104001, 2017.

Acknowledgements

Work supported in part by the US Department of Energy, Office of Science, Office of Fusion Energy Sciences DE-FG02-95ER54309, DE-FC02-04ER54698, and DE-SC0017992. Part of the data analysis was performed using the OMFIT integrated modeling framework.

Disclaimer

This report was prepared as an account of work sponsored by an agency of the United States Government. Neither the United States Government nor any agency thereof, nor any of their employees, makes any warranty, express or implied, or assumes any legal liability or responsibility for the accuracy, completeness, or usefulness of any information, apparatus, product, or process disclosed, or represents that its use would not infringe privately owned rights. Reference herein to any specific commercial product, process, or service by trade name, trademark, manufacturer, or otherwise does not necessarily constitute or imply its endorsement, recommendation, or favoring by the United States Government or any agency thereof. The views and opinions of authors expressed herein do not necessarily state or reflect those of the United States Government or any agency thereof.